

3D Magnetic Reconnection

Clare E. Parnell¹, Rhona C. Maclean¹, Andrew L. Haynes¹ and Klaus Galsgaard²

¹School of Mathematics & Statistics, University of St Andrews, North Haugh, St Andrews, Fife, KY16 9SS, UK
email: clare@mcs.st-and.ac.uk

²Niels Bohr Institute, Julie Maries vej 30, 2100 Copenhagen 0, Denmark

Abstract. Magnetic reconnection is an important process that is prevalent in a wide range of astrophysical bodies. It is the mechanism that permits magnetic fields to relax to a lower energy state through the global restructuring of the magnetic field and is thus associated with a range of dynamic phenomena such as solar flares and CMEs. The characteristics of three-dimensional reconnection are reviewed revealing how much more diverse it is than reconnection in two dimensions. For instance, three-dimensional reconnection can occur both in the vicinity of null points, as well as in the absence of them. It occurs continuously and continually throughout a diffusion volume, as opposed to at a single point, as it does in two dimensions. This means that in three-dimensions field lines do not reconnect in pairs of lines making the visualisation and interpretation of three-dimensional reconnection difficult.

By considering particular numerical 3D magnetohydrodynamic models of reconnection, we consider how magnetic reconnection can lead to complex magnetic topologies and current sheet formation. Indeed, it has been found that even simple interactions, such as the emergence of a flux tube, can naturally give rise to ‘turbulent-like’ reconnection regions.

Keywords. magnetic fields, (magnetohydrodynamics:) MHD

1. Introduction

Magnetic fields pervade pretty much all the objects in not only our solar system, but throughout the Universe. The strength and scales of complexity of the magnetic fields vary depending on the objects they are associated with. For instance, the magnetic fields emanating from the planets in our solar system are essentially dipolar in nature and are relatively weak compared to the magnetic field strengths that can be found on the Sun. Although at large distances the Sun’s magnetic field may be considered dipolar in nature, a closer look reveals that the Sun’s surface is threaded by a patchwork of features with fluxes ranging over many orders of magnitude through which magnetic fields are directed into, or out from, the Sun (Parnell *et al.* 2009). This magnetic patchwork is not static, but highly dynamic (Hagenaar *et al.* 2003; Thornton & Parnell 2010) and results in a very complex and dynamic evolution of the magnetic field and plasma throughout the solar atmosphere. One key type of behaviour that results from this dynamic complexity is the fundamental plasma physics process of magnetic reconnection. Magnetic reconnection is not unique to the solar atmosphere, but also plays a key role in a wide range of astrophysical phenomena such as, the heating of stellar coronae, the acceleration of stellar winds and astrophysical jets, the generation of magnetic fields via dynamo mechanisms and the creation of aurora and substorms in planetary magnetospheres.

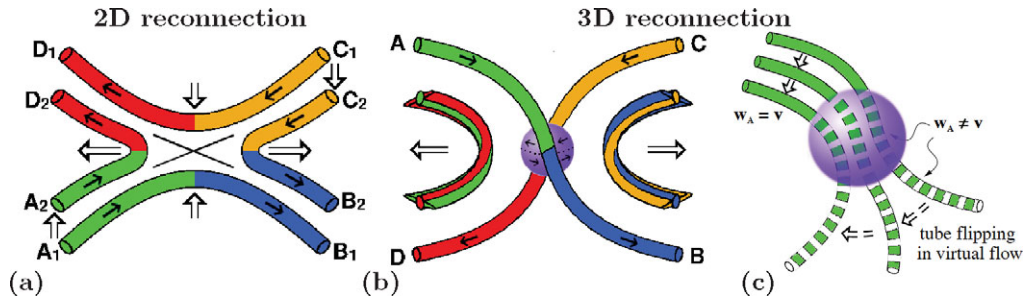


Figure 1. Illustrations highlighting the characteristics of (a) 2D and (b,c) 3D reconnection where the thick tubes represent flux tubes with arrows indicating the direction of the field, the block arrows represent the direction of the outflowing plasma and the purple shaded spheres are the diffusion volume in 3D with the arrows indicating the direction of plasma flow on its surface. (a) 2D reconnection at an X-type null point in which a pair of flux tubes A_1B_1 and C_1D_1 reconnect to form a new pair of flux tubes A_2D_2 and C_2B_2 . (b) 3D reconnection in which a pair of flux tubes AB and CD reconnect, but they do not form a new pair of flux tubes. (c) In 3D thin flux tubes reconnecting in a diffusion region will, on one side of the diffusion volume, appear to be moving slowly, but on the other side will appear to be moving incredibly fast. In reality the plasma on this side is moving just as slowly as it is on the other side, and this ‘virtual flow’ is simply a consequence of fieldlines changing connectivity within the diffusion region. Images derived from figures 2, 6 and 7 of Priest *et al.* (2003) and taken from Cargill *et al.* (2010).

2. Three-Dimensional Reconnection

Magnetic reconnection enables a magnetic field to globally restructure by locally changing the mapping of field lines. This process has a number of important consequences for the plasma as it converts free magnetic energy into three different types of energy. Local Joule heating at the reconnection site raises the internal energy of the plasma, bulk acceleration of the plasma from the reconnection site by the magnetic tension force of the newly formed field lines can produce large kinetic energies and finally the large electric fields found at the reconnection site accelerate particles throughout the diffusion region volume to high velocities.

Over the past fifty years the main focus of researchers has been on the two-dimensional (2D) aspects of magnetic reconnection, since this permits significant simplifications to be made to analytical and numerical problems (see, for example Priest & Forbes 2000; Biskamp 2000, for a review). However, it is now known three-dimensional (3D) reconnection has different characteristics to 2D reconnection and is a much richer and more varied process (Schindler *et al.* 1988; Hesse & Schindler 1988; Hesse 1995; Hornig & Priest 2003) (Fig. 1). Indeed, even a slight departure from an exactly 2D configuration leads to considerably different behaviour. Below the characteristics of 2D and 3D reconnection are compared and contrasted, before the wide variety of locations where 3D reconnection can occur are discussed.

2.1. Characteristics

In 3D, reconnection occurs in a range of locations that can, but do not have to be, associated with null points (points at which all components of the magnetic field are zero), unlike in 2D where reconnection can only occur at X-type null points (Fig. 1a). Reconnection in 3D occurs in a finite volume, known as a diffusion region, within which the plasma and the field lines become ‘unfrozen’, i.e., the plasma elements can move independently to the field lines (Fig. 1b). In this diffusion volume the field lines continually and

continuously diffuse through plasma and, as long as some portion of a field line is passing through the diffusion region volume, then it will reconnect with other field lines (Fig. 1c). Due to this behaviour it is not possible, in general, to find pairs of field lines that, after reconnection, match to form two new pairs of field lines, as occurs in 2D reconnection (c.f., Figs. 1a and 1b). Instead, it is only possible to find two surfaces (or volumes) of field lines that reconnect to form two new surfaces (or volumes). A consequence of reconnection throughout a finite volume is that the field line mappings are continuous, as opposed to discontinuous as they are in 2D reconnection.

2.2. Where can it occur?

A necessary and sufficient condition for 3D reconnection is that there exists a region where the ideal magnetohydrodynamic (MHD) assumption breaks down, i.e., a diffusion region through which

$$\int_{fl} \mathbf{E}_{||} dl \neq 0 ,$$

where fl is the field line path and $\mathbf{E}_{||}$ is the component of the electric field parallel to the field line (Schindler *et al.* 1988; Hesse & Schindler 1988; Hornig & Priest 2003). From the dot product of Ohm's law in MHD with the magnetic field, \mathbf{B} ,

$$\mathbf{E} \cdot \mathbf{B} + (\mathbf{v} \times \mathbf{B}) \cdot \mathbf{B} = \mathbf{j} \cdot \mathbf{B} / \sigma, \implies \mathbf{E}_{||} = \mathbf{j}_{||} / \sigma ,$$

where \mathbf{v} is the plasma velocity, \mathbf{j} is the electric current and σ is the electrical conductivity of the plasma. Hence, the presence of electric currents are essential for 3D reconnection, just as they are for 2D reconnection, but in 3D it is the parallel component of current that plays the crucial role. In 3D, strong accumulations of current and current layers, can arise in a wide variety of locations and are not just associated with magnetic nulls, as they are 2D.

The locations for current layer formation in 3D may be divided into those that are associated with *topological* features and those associated with *geometrical* features. Quasi separatrix layers (QSLs) are an example of a geometric feature about which reconnection can occur (Priest & Démoulin 1995; Démoulin *et al.* 1996; Titov *et al.* 2003; Aulanier *et al.* 2006; Titov 2007; Titov *et al.* 2009). QSLs are regions, usually long and narrow, identified on a plane in a magnetic domain which is threaded by field lines whose foot-points significantly diverge at one end. Naturally if two field lines which start off running along a similar path end up in very different places, as do QSL field lines, then these lines will be associated with electric currents. If the divergence of the field is dramatic then the associated currents may be significant and reconnection (termed either QSL or slip-running reconnection) may result (Aulanier *et al.* 2006). Many papers have been written where observed phenomena, such as flares, bright points and CMEs, have been explained using QSL reconnection (Aulanier *et al.* 2005; Aulanier *et al.* 2006; Aulanier *et al.* 2007; Masson *et al.* 2009; Pariat *et al.* 2009; Baker *et al.* 2009).

Currents also accumulate when magnetic flux tubes are twisted (Browning *et al.* 2008; Hood *et al.* 2009) or braided (Parker 1991; Galsgaard & Nordlund 1996; Longbottom *et al.* 1998; Wilmot-Smith *et al.* 2009, 2010; Pontin *et al.* 2011). Neither twisting nor braiding has to be excessive for strong currents to form, as is shown in the braiding experiments conducted by (Wilmot-Smith *et al.* 2010; Pontin *et al.* 2011) (Fig. 2). Their experiment consists of magnetic field that runs in the same direction, i.e., out from the bottom and into the top of the numerical box. The field is braided (Fig. 2a) and the initial force-free field involving this braid is associated with a large-scale current (Fig. 2b). However, as this force-free system is allowed to resistively relax, it first collapses to form intense

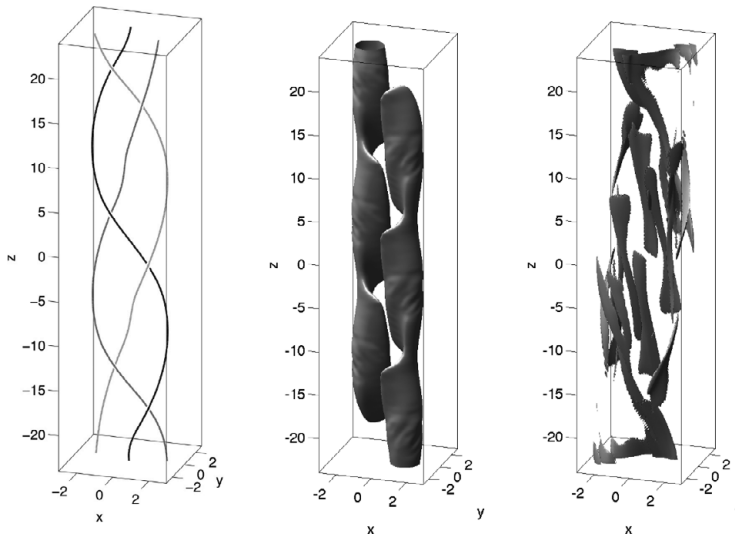


Figure 2. (a) Three sample magnetic field lines showing the force-free braiding structure of the initial magnetic field in the experiment of Pontin *et al.* (2011). (b) and (c) show isosurfaces of current at the start of the resistive relaxation and part way through once reconnection has started and fragmentation has broken up the current sheet providing rapid, long duration and widespread heating. Images taken from Pontin *et al.* (2011).

currents at which reconnection occurs leading to a cascade process in which the original large-scale homogeneous current fragments to smaller and smaller scales (Figs. 2c). This process is associated with rapid reconnection that occurs at multiple small-scale intense current accumulations throughout the domain. It is not simple for the magnetic field in this experiment to untangle itself and, since the plasma is not clever enough to work out the fastest way to untangle itself with the minimum amount of reconnection, magnetic flux is found to reconnect multiple times. This process of multiple reconnection was first observed by Parnell *et al.* (2009) and will be discussed in more detail in Section 3.3. The consequence of this type of behaviour is widespread reconnection throughout the flux tube, that lasts a long time. Hence, this 3D reconnection process can release a lot of energy in the whole of the flux tube over many hours and, hence, it may well be an important heating mechanism within the closed magnetic loop structures that fill the solar atmosphere.

3D magnetic null points are one type of topological feature which are prone to collapse to form a current layer, just like 2D nulls are. From a positive (negative) 3D null point (Fig. 3a) there are a set of field lines that extend out of (or into) the null forming what is known as a fan surface and a pair of field lines that extend into (out of) the null forming a curve known as the spine (e.g., Fukao *et al.* 1975; Lau & Finn 1990; Parnell *et al.* 1996). How the magnetic null is perturbed determines the nature of the collapse and the resulting current layer formed (Rickard & Titov 1996; Galsgaard & Nordlund 1997; Pontin *et al.* 2004; Pontin & Craig 2005; Pontin *et al.* 2005; Pontin *et al.* 2007; Priest & Pontin 2009). For instance, a rotational disturbance in planes perpendicular to the spine result in accumulations of current around the spine and/or fan. Two types of reconnection are found to be associated with these sorts of disturbances, namely, torsional-spine reconnection which occurs in response to a rotational disturbance of the fan plane, and torsional-fan reconnection which occurs in response to a rotational disturbance of the spine (Priest & Pontin 2009). However, the most common type of null-point reconnection

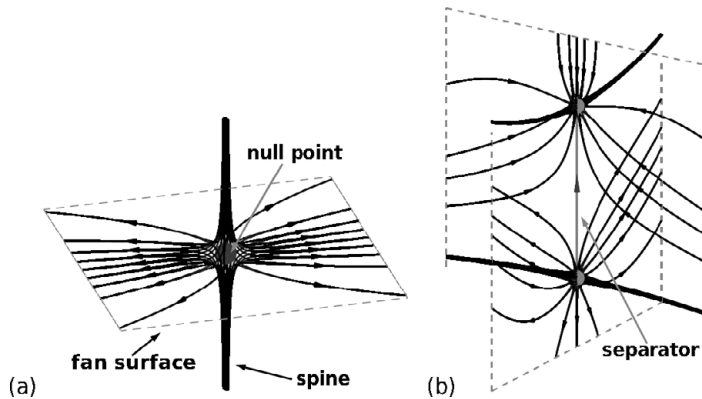


Figure 3. Magnetic field structure of (a) a positive 3D potential null point and (b) a separator formed by the intersection of two separatrix surfaces. Image taken from Pontin (2011).

tion, is spine-fan reconnection, which occurs as a result of any shearing motion in which the angle between the spine and fan are altered leading to a collapse of the spine and fan creating a current layer lying along both structures, (Pontin *et al.* 2007; Priest & Pontin 2009).

3D null points are not the only topological feature at which reconnection can occur. Fan surfaces from 3D nulls extend far out from the nulls themselves separating the magnetic field from topologically distinct field regions. Thus they are more generally known as separatrix surfaces and are bounded by either the edge of the domain investigated or by spine field lines from other nulls. If two separatrix surfaces intersect, special field lines called separators arise (Fig 3b). This manifestation of a separator is stable and resides at the intersection of four topologically distinct flux domains. This means they are in many ways the 3D equivalent of a 2D null point, although, of course, the magnetic field is only zero at the ends of the separators not along its length. It also means that reconnection at separators has global consequences and can lead to global restructuring of the magnetic field. In the following section, we focus on separator reconnection, in particular, we present examples showing how common separators are (Section 3.1), we discuss the nature of separator reconnection (Section 3.2) and consider the consequences of multiple separator reconnection (Section 3.3).

3. Separator Reconnection

3.1. Examples of Separator Reconnection

Determining the magnetic topology of a complex magnetic field is not trivial. Haynes & Parnell (2010) have recently published a method that can find the nulls, spines, separatrix surfaces and separators of magnetic fields that are known numerically on a discrete grid of points, or are known everywhere analytically. This method has been used successfully in a number of cases as discussed below.

Parnell *et al.* (2010b) analysed the magnetic topology of a flux tube emerging into an overlying coronal magnetic field from a 3D resistive MHD experiment (Archontis *et al.* 2005; Galsgaard *et al.* 2007). Although initially there were no null points in the region, when the flux tube rose up and started interacting with the overlying coronal magnetic field two clusters of magnetic nulls formed on either side of the emerged tube (Maclean *et al.* 2009). The clusters contain around 10-20 nulls most of which are short

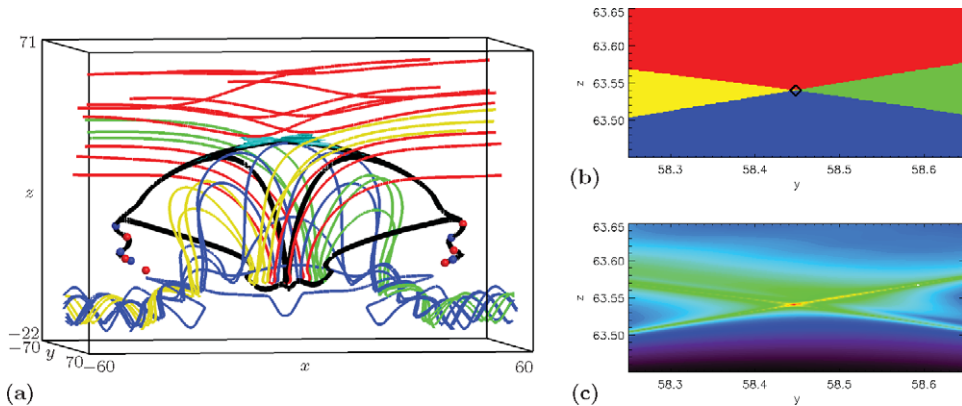


Figure 4. (a) Magnetic field structure at snapshot $109c_s$ during the emergence of a flux tube into an overlying coronal magnetic field. The positive/negative null points (red/blue spheres), separators (thick black lines), other fieldlines for context (overlying - red, flux tube - blue, flux tube to overlying - yellow and overlying to flux tube - green) and the strong regions of E_{\parallel} (30% of maximum - cyan isosurfaces) are shown. (b) Connectivity map in the plane $x = 0$ about the top arched inter-cluster separator showing flux domains coloured according to the connectivity of the fieldlines that thread them. The separator (black diamond) is located at the junction of four flux domains. (c) Contour plot of integrated E_{\parallel} along fieldlines threading the same region. The top arched separator threads the plane at the location of the maximum integrated E_{\parallel} indicating its importance for reconnection. Images taken from Parnell *et al.* (2010b).

lived, but a couple in each cluster are long lived and last throughout the duration of the interaction between the emerging and overlying flux regions. Parnell *et al.* (2010b) found that inside each cluster the nulls are connected by separators which form a chain of nulls. Between the two clusters there is one, or more usually many, separators that link the null clusters. These intercluster separators connect just one (or occasionally two) nulls from each cluster. These nulls are the long lived ones. Figs. 4a and 5a show a few magnetic field lines, all the separators and nulls at two times during the emergence of the tube and its interaction with the overlying field. In Fig. 4a, taken at time $109c_s$, there are 3 intercluster separators and 19 separators within the null clusters. Only one of the intercluster separators lies solely in the corona and threads the isosurface of \mathbf{E}_{\parallel} which indicates the main reconnection site. The other two intercluster separators initially rise up into the corona before dropping down under the emerging flux tube. This snapshot is taken during a relatively simple phase of the interaction. Fig. 5a is taken at an earlier time ($t = 86c_s$) during the most intense and dynamic phase of the reconnection. In this snapshot there are a total of 229 separators: 214 intercluster separators, which lie in the corona and all thread the large intense region of \mathbf{E}_{\parallel} (reconnection site), and 15 separators inside the null clusters. Figure 6a shows a view from above of the separators colour coded with \mathbf{E}_{\parallel} in this snapshot clearly highlighting the complex tangled mess formed by the intercluster separators.

All the separators reside at the intersection of the same four connectivities of flux. The two original flux domains (flux tube and overlying coronal field) and the two new flux domains which are created after reconnection (flux tube to overlying and overlying to flux tube). However, the separators do not all lie at the boundary between the same four flux domains. This is because flux of one connectivity may be divided into many topologically distinct flux domains, as explained by Parnell *et al.* (2008). The connectivity maps (Figs. 5b,c,d) show cuts through the mass of separators seen at $t = 86c_s$ and reveal the large number of distinct flux domains that have the same connectivity (same

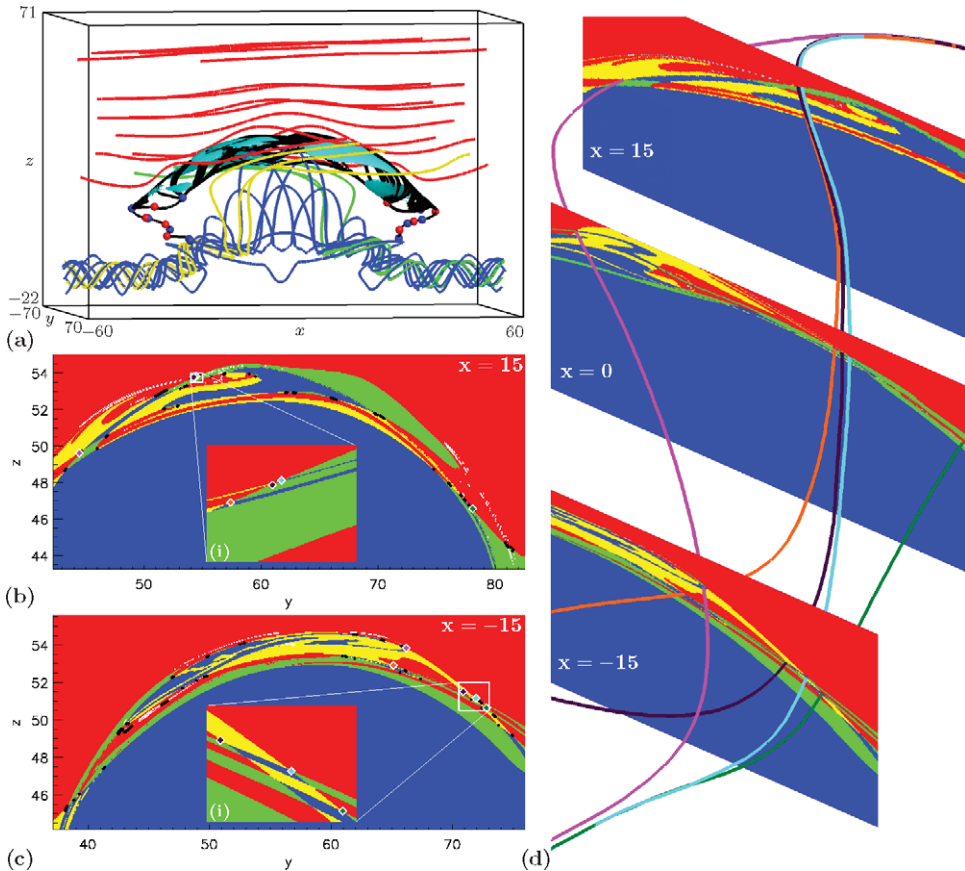


Figure 5. (a) Magnetic field structure at time $86c_s$ with the same features, indicated using the same nomenclature, as Figure 4. Connectivity maps in the (b) $x = 15$ and (c) $x = -15$ planes showing flux domains coloured according to field line connectivity. The separators (coloured and small black diamonds) are all located at the junctions of four flux domains. (d) Five separators are drawn threading connectivity maps plotted in 3 planes showing that separators may start out along similar paths before they diverge to follow very different paths. The coloured diamonds on (b) and (c) correspond to the coloured separators in (d). (b(i) and c(i)) Connectivity maps for the white boxed regions in (b) and (c), respectively. Images taken from Parnell *et al.* (2010b).

colour). Fig. 4b shows the connectivity map about the upper intercluster separator at $t = 109c_s$. One curious behaviour of separators is that they often start out along very similar paths before diverging at they move away from a null point at the end of the separators (Fig. 5d). This adds further to the difficulty of finding separators.

Furthermore, in all cases considered the isosurfaces of strong \mathbf{E}_{\parallel} are always threaded by separators, although a separator does not always have to thread a region of high \mathbf{E}_{\parallel} (see for example the isosurfaces in Figs. 4a and 5a). Fig. 6a shows a view from above of all the separators at $t = 86c_s$ colour coded according to the \mathbf{E}_{\parallel} along them. The red regions indicate strong \mathbf{E}_{\parallel} and thus these are likely to be the sites of strong reconnection. Fig. 6b shows a plot of the amount of reconnection (integral of the \mathbf{E}_{\parallel}) along all the separators shown in both Figs 4a and 5a against separator length. The intercluster separators are the long separators and the majority of them all show a significant amount of reconnection. The separators that are contained purely within the null clusters have no

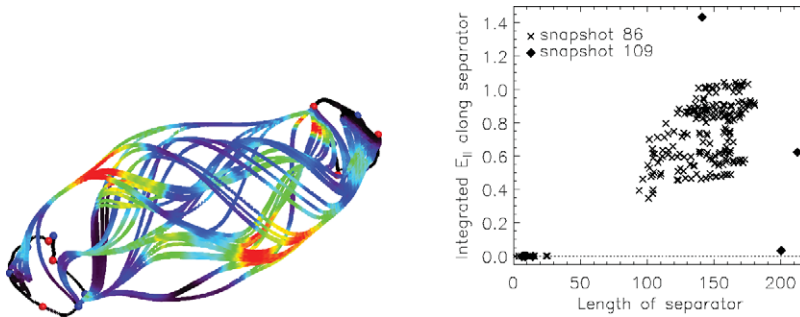


Figure 6. (a) View from above of the separators at time 86cs, colour coded according to the amount of \mathbf{E}_{\parallel} along them (where red indicates strong \mathbf{E}_{\parallel}). (b) A plot of integrated \mathbf{E}_{\parallel} along a separator against separator length. Images taken from Parnell *et al.* (2010b).

associated reconnection. This suggests that some, but not all, separators are important for reconnection.

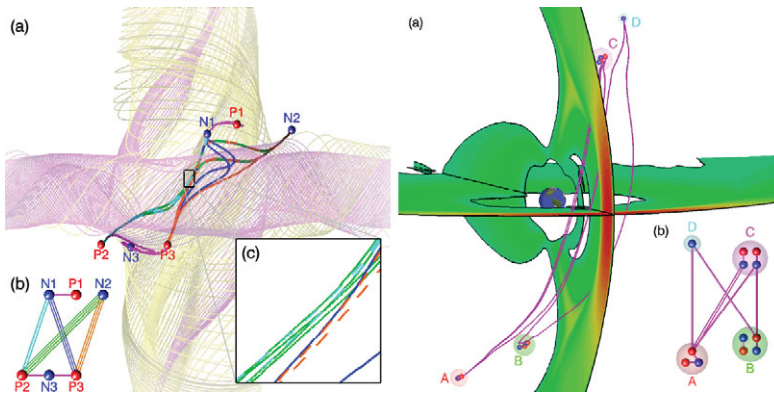


Figure 7. (a) 3D magnetic topology of the interaction, below the photosphere, between two emerging twisted flux tubes showing the null points (red and blue spheres), separators (thick lines), field lines of different connectivities (thin lines of different colours). The inset shows a close up of the separators. (b) Separators on the dayside of the magnetosphere for a Northwards interplanetary magnetic field of 45 degrees. Null points (red and blue spheres) and separators (thick lines) and pressure (filled contours). Examples taken from Haynes & Parnell (2010).

Fig. 7 shows sample snapshots of the magnetic topology from two other numerical MHD models. In each case examined so far the nulls have been found in clusters (as noted would occur by Albright 1999) and many separators have been found. It seems that, in general, pairs of nulls in the null clusters are linked by single separators and nulls with intercluster separators (separators linking the null clusters) are multiply connected nulls (i.e., they have many separators, as discussed in Parnell *et al.* 2008).

3.2. Nature of Separator Reconnection

A key question to answer is how does separator reconnection actually occur and why are some separators associated with reconnection whilst others are not?

In particular, Parnell *et al.* (2010a) focussed on answering the following key questions: Where are the enhanced regions of \mathbf{E}_{\parallel} along separators (i.e., where are the diffusion/reconnection regions)? How do these reconnection sites vary temporally and spatially along separators? What is the nature of the magnetic and velocity fields in the vicinity of a separator? The answers to these questions revealed that, locally, separator

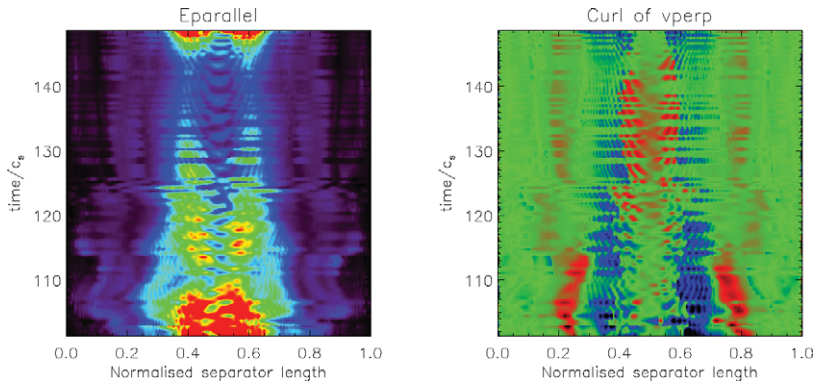


Figure 8. Temporal evolution of (a) \mathbf{E}_{\parallel} and (b) the curl of the velocity perpendicular to the longest lived intercluster separator from the flux emergence experiment investigated by (Parnell *et al.* 2010b). The x -axis is the normalised length of the separator and the y -axis is time in units of the sound travel time across the box (c_s). In (a) red represents strong \mathbf{E}_{\parallel} and in (b) blue/red represent negative/positive $\nabla \times \mathbf{v}_{\perp}$ (i.e. oppositely rotating plasma).

reconnection behaves very much like non-null reconnection as described by (Schindler *et al.* 1988; Hesse & Schindler 1988; Hesse 1995; Hornig & Priest 2003).

Parnell *et al.* (2010a) noted the following characteristics of separator reconnection. Here, though, we do not show the figures from their paper to illustrate the behaviour, but present new results determined from analysing the longest lived separator found in the flux emergence experiment considered by Parnell *et al.* (2010b). These results verify the characteristics found earlier by Parnell *et al.* (2010a) providing further support for their results. Regions of enhanced \mathbf{E}_{\parallel} are found to occur along the lengths of the separators, as opposed to at their end null points (Fig. 6a). This means that in separator reconnection the field lines do not in general reconnect at the nulls, but instead they reconnect within the vicinity of the middle of the separator. Moreover, the extent, strength and location of the diffusion regions change in time along the length of the separator (Fig. 8a). In fact, multiple diffusion regions seem to be quite common along individual separators (Figs. 6a and 8a).

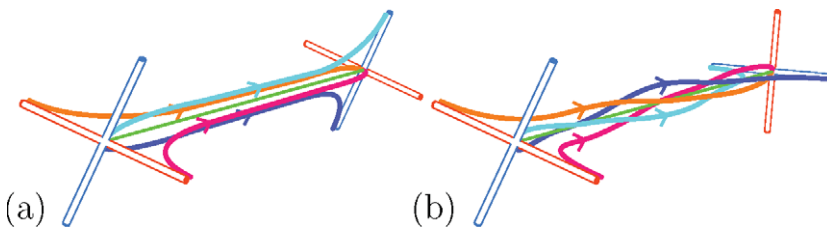


Figure 9. Cartoons showing the 3D global magnetic topology about (a) a separator with a hyperbolic local 3D field structure and (b) a separator with an elliptic local 3D magnetic field structure (equivalent to separator (a) twisted by $3\pi/2$). Each figure includes a separator (green), three field lines lying in the separatrix surface of the near null (blue, cyan, straight blue edge from near null) and three field lines lying in the separatrix surface of the far null (pink, orange, straight orange edge from far null), a spine from the near null (straight orange edge) and a spine from the far null (straight blue edge). Taken from Parnell *et al.* (2010a).

About a separator the magnetic field typically runs approximately parallel to the separator, but clearly, if there is a strong \mathbf{E}_{\parallel} about the separator, there must also be anti-parallel field perpendicular to it. Parnell *et al.* (2009) considered the magnetic field

perpendicular to the separator to investigate this component and found that this field does not have to be hyperbolic in nature, but can be elliptic (see Fig 9). The latter can result from a separator that has been twisted (Fig 9) or sheared.

In 2D reconnection, the magnetic field is carried into, and out of, the reconnection site by a stagnation type flow. In 3D reconnection scenarios, the magnetic field is obviously carried into the diffusion region and is also ejected out from the diffusion region (generally with high speed), however the inflow and outflow regions do not necessarily lie in a plane, and so the flow is not necessarily stagnation like. Additionally, a counter rotating plasma flow is found on either side of the diffusion region (Fig 8b). Such a flow is one of the main signatures of non-null reconnection Hornig & Priest (2003). The key reason that some separators are associated with reconnection, but others are not is because, in addition to a favourable magnetic field configuration for reconnection there must also be favourable plasma flows that drive the reconnection into these sites. If the flows about a separator are not driving magnetic flux in towards the separator then reconnection will not occur at that separator. However, note that in the flux emergence experiment of Parnell *et al.* (2010b) all the separators were created spontaneously at the onset of reconnection and did not exist before hand, so all were at sometime associated with reconnection, albeit in some cases only a very small amount.

3.3. Multiple Separator Reconnection

As already mentioned (and illustrated), multiple separators commonly arise in numerical 3D MHD experiments. This means that multiple reconnection sites also naturally arise (Haynes *et al.* 2007; Parnell *et al.* 2009; Wilmot-Smith *et al.* 2010; Pontin *et al.* 2011). Furthermore, in 3D, reconnection of current accumulations tends to cause the current to fragment into many smaller current layers where further reconnection occurs (Haynes *et al.* 2007; Hood *et al.* 2009; Wilmot-Smith *et al.* 2010; Parnell *et al.* 2010b; Pontin *et al.* 2011). That is, in 3D, reconnection often leads to a cascade in scales and, hence, turbulence.

One way to understand this type of behaviour is to realise that the plasma is not clever. It does not know the fastest way to untangle the magnetic field to release free magnetic energy and relax to a lower energy state. Instead, the plasma flows tend to squash the magnetic field together, accumulating currents, forming diffusion regions in which reconnection occurs. These reconnection sites squirt out newly reconnected field lines which result in further squashing of the field and current sheets forming off from the ends of the original diffusion regions. At these sites, more reconnection occurs and more current sheets are formed, etc. This occurs because the first reconnection of field lines is, in general, unlikely to be the most optimum for untangling the field. So the newly reconnected flux finds itself still tangled and must reconnect again and again before it is untangled. This type of behaviour was first noticed by Haynes *et al.* (2007) and was explained by Parnell *et al.* (2009). However, it has now been found in many different experiments (e.g., Haynes *et al.* 2007; Dorelli & Bhattacharjee 2008; Hood *et al.* 2009; Wilmot-Smith *et al.* 2010; Pontin *et al.* 2011). This behaviour was originally described by Parnell *et al.* (2009), who named it recursive reconnection, however, a better name is probably multiple reconnection.

In cases of multiple reconnection, the same flux may be reconnected multiple times, as the case suggests. Parnell *et al.* (2009) found that in their experiment the flux was reconnected 1.8 times more than it would have been if the flux was only reconnected once and the fastest untangling had occurred. This behaviour has also be found in other experiments. For instance, Pontin *et al.* (2011) studied how much reconnection occurred in the braiding experiment of Wilmot-Smith *et al.* (2010). They found that the flux in

their experiment must have reconnected 1.6 times implying that the many reconnection sites that they found were multiply reconnecting the magnetic field.

The multiple reconnection of magnetic field at many different diffusion regions has some interesting consequences for the energetic behaviour of the plasma. In particular, the energy release (i) is wide spread as it occurs at multiple sites, (ii) occurs for longer as the magnetic field does not take the simplest and fastest path to untangle and (iii), in cases of driven reconnection, more energy is released than in the potential case. This happens because in the cases of multiple reconnection more Poynting flux can be injected into the system and hence more energy can be released.

4. Discussion

In this review, the complexities of 3D magnetic fields and 3D magnetic reconnection have been highlighted. The main differences between 2D and 3D reconnection have been discussed. Although 3D reconnection can occur in a wide range of locations the actual nature of the reconnection is very similar in all the cases of non-null reconnection, including separator reconnection. Although, separators are special field lines that link two null points, the null points themselves play no real role in separator reconnection and hence the reconnection at them is of non-null type.

A series of examples have been shown of globally complex 3D magnetic topologies that arise in a range of astrophysical magnetic fields. In all of these examples a multitude of separators are found and each reconnection site (region of strong \mathbf{E}_{\parallel}) within the models has, so far, always been found to be threaded by one or more separators. In all the resistive MHD experiments discussed the magnetic field is found to become locally very complex upon the initiation of magnetic reconnection. That is to say, following the onset of reconnection, macroscopic current regions have a tendency to fragment into a multi-scale array of current layers at each of which reconnection occurs. This turbulent like behaviour enables the process of 3D reconnection to be widespread and longer lasting (due to the multiple reconnection of flux) than one might imagine. This therefore, means that reconnection is a very good candidate for heating solar and stellar coronae. By managing to reconnect flux at multiple sites over a large area a lot of flux may be processed in a short space of time and hence reconnection can also release sufficient free energy rapidly enough to power a solar flare.

References

- Albright, B. J. 1999, *Phys. Plasmas*, 6, 4222
- Archontis, V., Moreno-Insertis, F., Galsgaard, K., & Hood, A. W. 2005, *Astrophys. J.*, 635, 1299
- Aulanier, G., Golub, L., DeLuca, E. E., *et al.* 2007, *Science*, 318, 1588
- Aulanier, G., Parlat, E., & Démoulin, P. 2005, “*Astron. Astrophys.*”, 444, 961
- Aulanier, G., Parlat, E., Démoulin, P., & Devore, C. R. 2006, *Solar Phys.*, 238, 347
- Baker, D., van Driel-Gesztelyi, L., Mandrini, C. H., Démoulin, P., & Murray, M. J. 2009, “*Astrophys. J.*”, 705, 926
- Biskamp, D. 2000, *Magnetic Reconnection in Plasmas* (Cambridge, UK: Cambridge University Press)
- Browning, P. K., Gerrard, C., Hood, A. W., Kevis, R., & van der Linden, R. A. M. 2008, *Astron. Astrophys.*, 485, 837
- Cargill, P., Parnell, C., Browning, P., de Moortel, I., & Hood, A. 2010, *Astronomy and Geophysics*, 51, 030000
- Démoulin, P., Henoux, J. C., Priest, E. R., & Mandrini, C. H. 1996, *Astron. Astrophys.*, 308, 643

- Dorelli, J. C. Bhattacharjee, A. 2008, *Physics of Plasmas*, 15, 056504
- Fukao, S., Ugai, M., & Tsuda, T. 1975, *Report Ionosphere Space Research Japan*, 29, 133
- Galsgaard, K., Archontis, V., Moreno-Insertis, F., & Hood, A. W. 2007, *Astrophys. J.*, 666, 516
- Galsgaard, K. Nordlund, Å. 1996, *J. Geophys. Res.*, 101, 13445
- Galsgaard, K. Nordlund, Å. 1997, *J. Geophys. Res.*, 102, 231
- Hagenaar, H. J., Schrijver, C. J., & Title, A. M. 2003, *Astrophys. J.*, 584, 1107
- Haynes, A. L. Parnell, C. E. 2010, *Physics of Plasmas*, 17, 092903
- Haynes, A. L., Parnell, C. E., Galsgaard, K., & Priest, E. R. 2007, *Royal Society of London Proceedings Series A*, 463, 1097
- Hesse, M. 1995, in *Reviews in Modern Astronomy*, ed. G. Klare, *Reviews in Modern Astronomy*, 8, 323
- Hesse, M. Schindler, K. 1988, *J. Geophys. Res.*, 93, 5559
- Hood, A. W., Browning, P. K., & van der Linden, R. A. M. 2009, *Astron. Astrophys.*, in press
- Hornig, G. Priest, E. R. 2003, *Phys. Plasma*, 10, 2712
- Lau, Y. Finn, J. M. 1990, *Astrophys. J.*, 350, 672
- Longbottom, A. W., Rickard, G. J., Craig, I. J. D., & Sneyd, A. D. 1998, *Astrophys. J.*, 500, 471
- Maclean, R. C., Parnell, C. E., & Galsgaard, K. 2009, *Solar Phys.*, 260, 299
- Masson, S., Parlat, E., Aulanier, G., & Schrijver, C. J. 2009, *Astrophys. J.*, 700, 559
- Parlat, E., Masson, S., & Aulanier, G. 2009, "*Astrophys. J.*", 701, 1911
- Parker, E. N. 1991, in *Mechanisms of Chromospheric and Coronal Heating*, ed. P. Ulmschneider, E. R. Priest, & R. Rosner, 615
- Parnell, C. E., DeForest, C. E., Hagenaar, H. J., *et al.* 2009, *Astrophys. J.*, 698, 75
- Parnell, C. E., DeForest, C. E., Hagenaar, H. J., Lamb, D. A., & Welsch, B. T. 2008, in *First Results From Hinode*, eds. S. A. Matthews, J. M. Davis, & L. K. Harra, *Astronomical Society of the Pacific Conference Series*, 397, 31
- Parnell, C. E., Haynes, A. L., Galsgaard, K. 2010a, *J. Geophys. Res. (Space Physics)*, 115, 2102
- Parnell, C. E., Maclean, R. C., Haynes, A. L. 2010b, *Astrophys. J. Letts.*, 725, L214
- Parnell, C. E., Smith, J. M., Neukirch, T., & Priest, E. R. 1996, *Physics of Plasmas*, 3, 759
- Pontin, D. I. 2011, "*Adv. Space Res.*"
- Pontin, D. I., Bhattacharjee, A., & Galsgaard, K. 2007, *Physics of Plasmas*, 14, 052106
- Pontin, D. I. Craig, I. J. D. 2005, *Physics of Plasmas*, 12, 072112
- Pontin, D. I., Hornig, G., & Priest, E. R. 2004, *Geophysical and Astrophysical Fluid Dynamics*, 98, 407
- Pontin, D. I., Hornig, G., & Priest, E. R. 2005, *Geophys. Astrophys. Fluid Dynamics*, 99, 77
- Pontin, D. I., Wilmot-Smith, A. L., Hornig, G., & Galsgaard, K. 2011, *Astron. Astrophys.*, 525, A57+
- Priest, E. R. Démoulin, P. 1995, *J. Geophys. Res.*, 100, 23443
- Priest, E. R. Forbes, T. G. 2000, *Magnetic reconnection* (Cambridge, UK: Cambridge University Press)
- Priest, E. R., Hornig, G., & Pontin, D. I. 2003, *J. Geophys. Res.*, 108, 1285
- Priest, E. R. Pontin, D. I. 2009, *Physics of Plasmas*, 16, 122101
- Rickard, G. J. Titov, V. S. 1996, *Astrophys. J.*, 472, 840
- Schindler, K., Hesse, M., & Birn, J. 1988, *J. Geophys. Res.*, 93, 5547
- Thornton, L. M. Parnell, C. E. 2010, *Solar Phys.*, 220
- Titov, V. S. 2007, *Astrophys. J.*, 660, 863
- Titov, V. S., Forbes, T. G., Priest, E. R., Mikić, Z., & Linker, J. A. 2009, "*Astrophys. J.*", 693, 1029
- Titov, V. S., Galsgaard, K., & Neukirch, T. 2003, *Astrophys. J.*, 582, 1172
- Wilmot-Smith, A. L., Hornig, G., & Pontin, D. I. 2009, *Astrophys. J.*, 696, 1339
- Wilmot-Smith, A. L., Pontin, D. I., & Hornig, G. 2010, *Astron. Astrophys.*, 516, A5+